Development 134, 3905-3915 (2007) doi:10.1242/dev.008276

The *C. elegans* CBFβ homologue BRO-1 interacts with the Runx factor, RNT-1, to promote stem cell proliferation and self-renewal

Hiroshi Kagoshima[1,*,†], Rachael Nimmo[2,*], Nicole Saad[2], Junko Tanaka[3], Yoshihiro Miwa[3,4], Shohei Mitani[5], Yuji Kohara[1] and Alison Woollard[2,†]

In this report, we investigate the *C. elegans* CBFβ homologue, BRO-1. *bro-1* mutants have a similar male-specific sensory ray loss phenotype to *rnt-1* (the *C. elegans* homologue of the mammalian CBFβ-interacting Runx factors), caused by failed cell divisions in the seam lineages. Our studies indicate that BRO-1 and RNT-1 form a cell proliferation-promoting complex, and that BRO-1 increases both the affinity and specificity of RNT-1-DNA interactions. Overexpression of *bro-1*, like *rnt-1*, leads to an expansion of seam cell number and co-overexpression of *bro-1* and *rnt-1* results in massive seam cell hyperplasia. Finally, we find that BRO-1 appears to act independently of RNT-1 in certain situations. These studies provide new insights into the function and regulation of this important cancer-associated DNA-binding complex in stem cells and support the view that Runx/CBFβ factors have oncogenic potential.

KEY WORDS: *C. elegans*, *CBFβ*, Stem cell, Proliferation, Self-renewal, Runx

INTRODUCTION

CBF, or PEBP2, is a heterodimeric DNA binding complex, composed of an α subunit (CBFα/PEBP2α, now known as Runx) and a β subunit (CBFβ/PEBP2β). CBFβ has been shown to enhance the DNA binding affinity and stability of Runx proteins and is required for many of their in vivo functions (Adya et al., 2000; Huang et al., 2001). There are three mammalian Runx genes, *Runx1*, *Runx2* and *Runx3*, whereas *C. elegans* contains a single Runx orthologue, *rnt-1* (Kagoshima et al., 2005; Nam et al., 2002; Nimmo et al., 2005). Runx factors act as activators or repressors of transcription, depending on the context in which they bind to DNA (Canon and Banerjee, 2003; Stein et al., 2004), and have central roles in cell fate determination and differentiation during development (reviewed by Coffman, 2003). In addition, Runx genes have been postulated to act both as tumour suppressors and oncogenes (reviewed by Cameron and Neil, 2004). CBFβ gene rearrangements are also associated with cancer (Adya et al., 1998; Lutterbach et al., 1999).

RNT-1 (the single *C. elegans* Runx orthologue), is required for the correct division pattern in the stem cell-like, lateral hypodermal seam cell lineages (Nimmo et al., 2005; Kagoshima et al., 2005) (reviewed by Kagoshima et al., 2007). Seam cells have stem-like properties as they undergo self-renewal and expansion whilst producing differentiated cells. They divide asymmetrically at the beginning of each larval stage (larval stages L1 through L4 – distinct developmental stages separated by a molt), producing another seam cell that will continue to proliferate and a hypodermal nucleus that differentiates and fuses with the main hypodermal syncytium (Sulston and Horvitz, 1977). In addition, at the start of L2 and in a male-specific developmental programme in L3, seam cells undergo expansion via symmetrical division (Sulston et al., 1980). In males, these extra seam cells eventually give rise to ray precursor cells from which the sensory rays are derived (Sulston et al., 1980). Seam stem cells can therefore be regarded as pluripotent as they contribute a number of cell types during postembryonic development. *rnt-1* mutant males lack the correct number of sensory rays as a result of variable seam cell division failures during larval development (Nimmo et al., 2005). By contrast, ectopic expression of *rnt-1* results in seam cell hyperplasia (Nimmo et al., 2005).

In this report, we show, in contrast to previous suggestions (Adya et al., 2000), that *C. elegans* does indeed contain a functional CBFβ homologue, BRO-1. *bro-1* was originally identified as a likely CBFβ orthologue by Lee and colleagues (Lee et al., 2004). We find that *bro-1* deletion mutants have a very similar male tail phenotype to *rnt-1*, suggesting the two genes interact, although we also observe unprecedented RNT-1-independent BRO-1 functions. We find that BRO-1 acts not only to increase the affinity of RNT-1 for DNA but also to dramatically increase the specificity of RNT-1-DNA interactions. Overexpression of *bro-1* increases the number of seam cells by causing supernumerary seam cell divisions, as well as preventing asymmetric daughters from adopting the hypodermal fate. Furthermore, when *bro-1* and *rnt-1* are co-overexpressed, massive seam cell hyperplasia results. This work complements and extends analyses of Runx/CBFβ function in other systems, making *C. elegans* a premier model system for the further study of these important cancer-associated genes, especially in the context of stem cell lineages.

MATERIALS AND METHODS

Strains and *C. elegans* maintenance

All strains used were derived from the wild-type (WT) Bristol strain N2. Worm manipulations were performed as previously described (Sulston and Hodgkin, 1988).

[1]Genome Biology Laboratory, National Institute of Genetics, Mishima 411-8560, Japan. [2]Genetics Unit, Department of Biochemistry, University of Oxford, South Parks Road, Oxford OX1 3QU, UK. [3]Graduate School of Comprehensive Human Sciences, University of Tsukuba, Tsukuba 305-8577, Japan. [4]Precursory Research and Embryonic Science and Technology (PRESTO), JST, Okazaki 444-8585, Japan. [5]Department of Physiology, Tokyo Women's Medical University School of Medicine, Tokyo 162-8666, Japan.

*These authors contributed equally to this work
†Author for correspondence (e-mail: hkagoshi@lab.nig.ac.jp; alison.woollard@bioch.ox.ac.uk)

Accepted 20 August 2007

bro-1 alleles

bro-1 deletion alleles *tm1183*, *tm1229* and *tm658* were isolated from trimethylpsoralen/ultraviolet (TMP/UV) mutagenesis screens (Gengyo-Ando and Mitani, 2000) by the Japanese deletion consortium (National Bioresource Project for the Experimental Animal 'Nematode C. elegans', http://shigen.lab.nig.ac.jp/c.elegans/index.jsp). Deletion strains were backcrossed to WT ten times before analysis.

Lineage analysis

Worms were mounted for lineage analysis and observed as previously described (Nimmo et al., 2005). Hypodermal nuclei were distinguished from neuronal nuclei on the basis of their appearance: hypodermal nuclei look like 'fried eggs' with a large nucleolus, whereas neuronal nuclei are smaller and more granular, with a less distinct nucleolus.

Transgenic worms

Injections were performed (using 20-100 ng/μl DNA) as previously described (Mello and Fire, 1995), using transformation markers *rol-6(su1006)* or *dpy-20*$^{+}$ (pMH86). Where appropriate, transgenic arrays were integrated using UV irradiation (Mitani, 1995). Integrated strains were backcrossed twice with WT before use.

GFP/RFP reporter constructs

The *bro-1::GFP* rescuing reporter construct, pHK196, was made by amplifying a 2.5 kb fragment of cosmid F56A3 (15071-17586 nt) with primers beta-1 (ggaaagGGATCCctcatcgagaaatcagtccaattt cg) and beta-3 (gaatctGGTACCcaaatgggaagaccatcgcgtcgaagg) and cloning into the *Kpn*I-*Bam*HI fragment of GFP reporter vector pPD95.79 (http://www.addgene.org/Fire_Lab). The *bro-1::RFP* rescuing construct pHK328 (*bro-1::mRFP)* was made by substituting monomeric RFP for GFP in pHK196. In addition, a *bro-1::DsRed* rescuing construct, pAW303 was also made, by the PCR-fusion based method (Hobert, 2002), amplifying *dsRed* from plasmid pHC183 (a kind gift from Neline Kriek) using primers NS45 (atggcctcctccgagaacgtcatc) and NS46 (aagggcccgtacggccactagtagg) and *bro-1*from plasmid pAW272 using primers NS19 (ctcgtaaatcgacacaaatgc) and NS17 (gatgacgttctcggaggaggccatAATGGGAAGACCATCGCG). The sewing reaction was performed using nested primers NS20 (tcaaatatg-ttgcgctgtacg) and NS47 (ggaaacagttatgtttggtatattggg) and the PCR product cloned into the TOPO-2.1 vector (Invitrogen) to make pAW303. The *rnt-1::GFP* constructs used in this work, pAW260 and pHK192 have been previously described (Kagoshima et al., 2005; Nimmo et al., 2005). The seam cell-specific marker, *SCM::GFP* (strain JR667) was used to assay seam cell number (*unc-119 (e2498::Tc1III); wIs51[SCM::GFP + unc*-119*]*. A *dpy-7::GFP* reporter strain (*ijIs12)* (a kind gift from Iain Johnstone) was used as a hypodermal marker.

RNAi

PCR of *cki-1* for dsRNA synthesis was performed as previously described (Nimmo et al., 2005). dsRNA was synthesised from gel-purified PCR product and injected as previously described (Fire et al., 1998).

RT-PCR

Total RNA was extracted from a 100 μl pellet of synchronised L1 larvae using the hot phenol method (Furger et al., 2001). RT-PCR was then performed as previously described (Pocock et al., 2004) using gene-specific primers. *rnt-1*: RN70 (ctaacgcctgttccagataatac) and RN81 (ggagatg-ataggcatgtagacg). *bro-1:*RN104 (aaagaacgacaacggaccag) and RN105 (atttcagcatccgtcagtcc). *ama-1*: RN102 (tgtctcacgcgttcagtttg) and RN103 (aatttccagcactcgaggag).

RUBY assay

The Runt domain of RNT-1 and BRO-1 were fused to the C terminus of DsRed1 with linker amino acid sequences (GSTSGSGKPGSGEGSTKPG) in an EBV-based vector, pEB6CAG-MCS (Tanaka et al., 1999). HEp-2 cells in 24-well dishes were transfected with 0.5 μg of the plasmid DNAs using TransFectin (Bio-Rad) and cultured in the presence of 1 mg/ml G418 (RUBY-RNT-1RD) or 100 μg/ml Zeocin (RUBY-BRO-1) or both (co-transfection) Cells were used 4 days later for flow cytometry and fluorescent microscopic observation. For the positive and negative control data shown in the supplementary figure (see Fig. S1 in the supplementary material), DNA fragments encoding the Runt domain of Runx2, the mutated version G151R, and CBFβ, were subcloned into pEB6CAG-WR1-SRZ to yield vectors expressing RUBY-wtRunx2-RD, RUBY-G151RRunx2-RD and RUBY-CBFβ.

Protein purification

The wild-type and mutant Runt domains of *C. elegans* RNT-1 were produced as fusions with N-terminal glutathione S-transferase (GST) and hexahistidine (6xHis) tags. The wild-type Runt domain (amino acids 10-137) was amplified by PCR using the cDNA template yk309f5 and the primers, 5′RD (cgcggtaccCCATGGcatatgagaggatcgcatcaccatcaccatcacgg-atccatgaccaacgtcttccatcacgttcgg), 3′RD (cgcgaattcTGTACAtcattgtggt-tttggtattctcgcatccc). The mutant Runt domain, containing a missense mutation ($I_{112}K$) corresponding to *rnt-1(e1241)*, was generated by PCR using the primers, 5′RD, 3′RD and e1241-5 (cgccgaatgtTtaacgattgtcaaatg-gaattttcg), e1241-3 (gacaatcgttaAacattcggcgccgatgatggtgg). PCR products were cloned into the *Nco*I-*Bsr*GI site of the vector pDEST15 (Clontech). BRO-1 was produced as a C-terminal 6xHis-tagged protein. The entire BRO-1 coding sequence was amplified by PCR using the cDNA clone yk211f2 and the primers, N-BRO-1 (cttggtgcatgcCTGCAGacatgaaaagaa-cgacaacggaccagc) and C-BRO-1 (taaaagggatcccCTCGAGaatgggaagacca-tcgcgtcgaagg), and was cloned into the *Pst*I-*Xho*I site of a T7-expression vector derived from pHIT12 (Keefe et al., 2001) (H. Tabara, personal communication). All 6xHis-tagged proteins were expressed in the BL21 strain of *Escherichia coli*.

Since the Runt domain fusion proteins were expressed as inclusion bodies, the harvested cells were incubated in solubilization buffer (0.1 M sodium phosphate, 10 mM Tris, 6 M guanidine-HCl, 1 mM phenylmethylsulfonyl fluoride, 10 mM β-mercaptoethanol and 0.1% Nonidet P-40, pH 8.0) and purified on a Ni-NTA resin (Qiagen). Purified proteins were renatured by stepwise dialysis at 4°C against 100 volumes of dialysis buffers (0.1 M sodium phosphate,10 mM Tris, 50 mM glycine, 2 mM β-ME, 0.1% NP-40 and 20% glycerol, pH 8.0) containing 4 M, 2 M and 0 M guanidine-HCl, respectively, for 4 hours or overnight. BRO-1-6xHis was purified as a soluble protein on the Ni-NTA resin.

Electrophoretic mobility shift assay (EMSA)

For the preparation of the probe and competitors, synthetic oligonucleotides [WT: RUNX-WT-1 (catgactgctAACCGCAgatgac) and RUNX-WT-2 (gtacgtcatcTGCGGTTagcagt), and Mut: RUNX-Mut-1 (catgactgct-AATCGAAgatgac) and RUNX-Mut-2 (gtacgtcatcTTCGATTagcagt)] were annealed and extended by a standard Klenow fragment reaction with [α-^{32}P]dATP, without radioisotope for competitors. The DNA binding reaction (final volume, 10 μl) was carried out at 25°C for 30 minutes in EMSA buffer (20 mM HEPES-KOH, 4% Ficoll, 2 mM EDTA, 1 mM DTT, 100 mM KCl, 6% glycerol, 0.2 mg/ml bovine serum albumin, 0.04% Bromphenol Blue and 10 fmol of labelled probe, pH 7.4). The reaction mixture was loaded on a 10% nondenaturing polyacrylamide gel in 0.25×TBE and electrophoresed at 4°C.

RESULTS

bro-1 mutants have missing rays as a result of failures in V and T lineage divisions

The BRO-1 protein sequence is 19% identical (36% similar) to human CBFβ (Fig. 1) (reviewed by Kagoshima et al., 2007). In addition to the low overall homology, it also lacks the conserved region in fly and mammalian CBFβ corresponding to the sequences between the beta sheets, β3 and β6, which might be expected to interfere with the positioning of the Runx interaction domain around β3 and β5 (Tahirov et al., 2001) (Fig. 1B). Three deletion alleles of *bro-1* are available, *tm658*, *tm1183* and *tm1229* (Fig. 1). *tm1183* and *tm1229* are presumed null alleles and *tm1183* has been used throughout this study. Ray and seam cell phenotypes in *bro-1(tm1183)* animals are shown in Fig. 2. *bro-1(tm1183)* animals typically lack five rays from each side of the male tail (Fig. 2C,D)

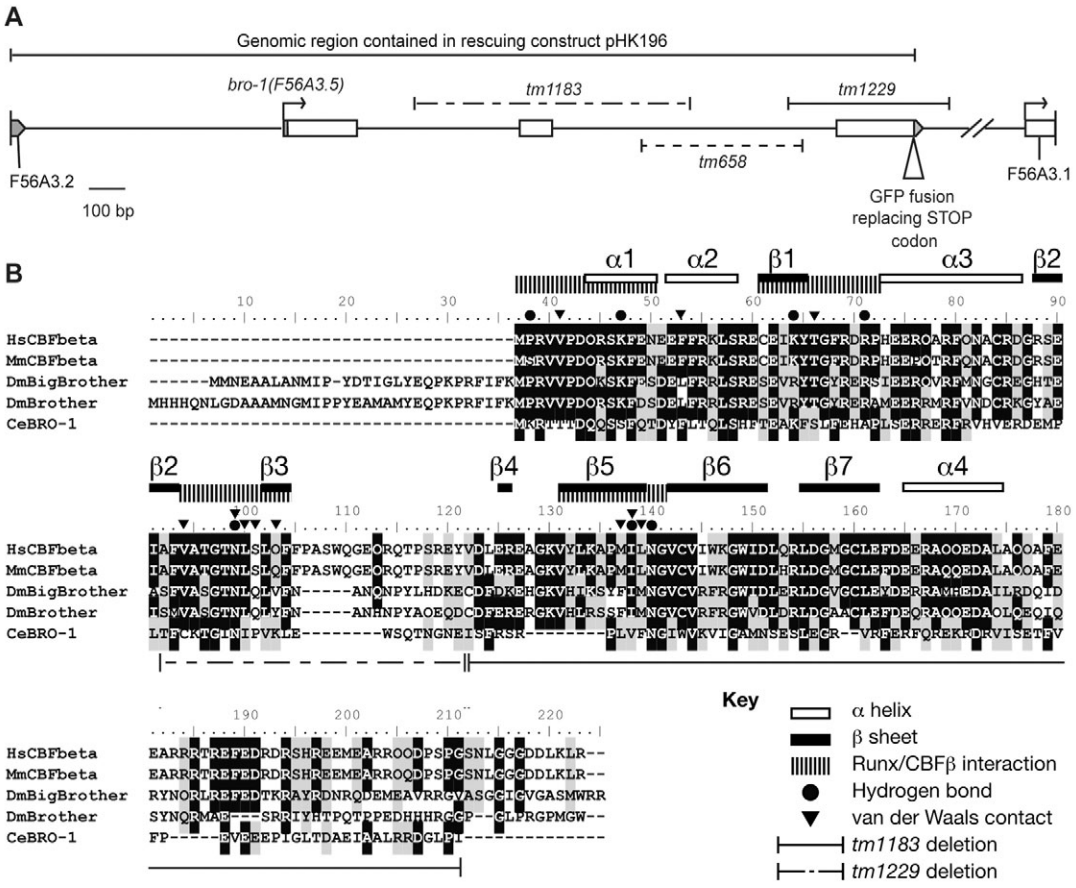

Fig. 1. *bro-1* is a *CBFβ* orthologue. (**A**) Genomic structure of the *bro-1* gene and the region contained in the rescuing construct pHK196. (**B**) Alignment of BRO-1 and CBFβ orthologues from *Drosophila* (Brother, NP477066.2 and Big brother, NP477065.3), mouse (NP071704.2) and human (isoform 1, NP074036.1). Identical amino acids are shown on a black background; similar amino acids are on a grey background. The secondary structure profiles determined for mouse CBFβ (open box, α helix; black box, β sheet) are shown on the top of the alignment (Tahirov et al., 2001), indicating the RUNX1-interacting regions, and including the particular amino acids that would be expected to participate in the direct interaction.

and the phenotype is identical in *tm1229* (data not shown). Both V- and T-derived rays are variably missing. *tm658* has no obvious phenotype (data not shown) but lacks only intronic sequences. The *bro-1* ray-loss phenotype is very similar to loss-of-function *rnt-1* alleles (Fig. 2B) (Kagoshima et al., 2005; Nimmo et al., 2005) and is completely rescued in transgenic worms carrying a full-length genomic *bro-1* construct (pHK193; Fig. 2D). *bro-1* animals have fewer seam cells than WT (Fig. 2E). A representative V and T lineage trace of *bro-1(tm1183)* animals from late L1 up to mid L3 is shown in Fig. 2F,G. Various seam division failures are evident.

In addition, a representative L1 T lineage of *bro-1(tm1183)* animals is shown in Fig. 2H, in which daughters of the posterior branch T.p often fail to give rise to phasmid neurons. This gives rise to a dye-filling defect (Dyf phenotype) in *bro-1* mutant animals (data not shown). Identical T lineage L1 defects in *rnt-1* animals have been described previously, and explained as the loss of the characteristic asymmetry of the first T blast cell division (Kagoshima et al., 2005). In WT animals, T divides to give two daughters, T.a and T.p (Fig. 2H). T.a goes on to produce hypodermal daughters whereas T.p normally produces neurons. Thus the two branches of the T lineage are thought of as asymmetric. In *rnt-1* mutants, it has previously been argued that since the daughters of T.p (the T.px cells) have a hypodermal rather than a neuronal morphology, the asymmetry of the T division is lost (Kagoshima et al., 2005). The same defect was observed in *bro-1* mutants (Fig. 2J,L). However, this defect could be a consequence of cell cycle arrest. It has been previously shown that the nuclei of the T.p daughter cells look hypodermal in WT soon after they are born (Fig. 2I) (Sulston and Horvitz, 1977) and we have confirmed their hypodermal characteristics using the hypodermal-specific marker *dpy-7::GFP* (Fig. 2K). These data suggest that the neuronal fate is normally acquired gradually over time. In WT animals, commitment to subsequent divisions, or at least progress through the cell cycle, may be required to commit to a distinct neuronal fate. In *bro-1* (and *rnt-1*) animals, however, these subsequent divisions do not always occur, and thus hypodermal characteristics are retained. However, in the absence of a suitable neuronal marker, it is difficult to exclude the possibility that RNT-1 and BRO-1 may be required in some other way for the acquisition of neuronal identity, for instance directly, by regulating asymmetry of the T blast cell division, as opposed to indirectly, by programming further cell proliferation.

The phenotype of *bro-1 rnt-1* double mutant animals is shown in Fig. 3. These animals have a very similar male tail phenotype to either single mutant (Fig. 3B,E), suggesting that the two genes act in a common pathway. Given their sequence homologies, it is likely that RNT-1 and BRO-1 form a DNA binding complex. However, the L2-L3 V lineage trace shown in Fig. 3C indicates that the penetrance of division defects is slightly higher in double mutant animals than

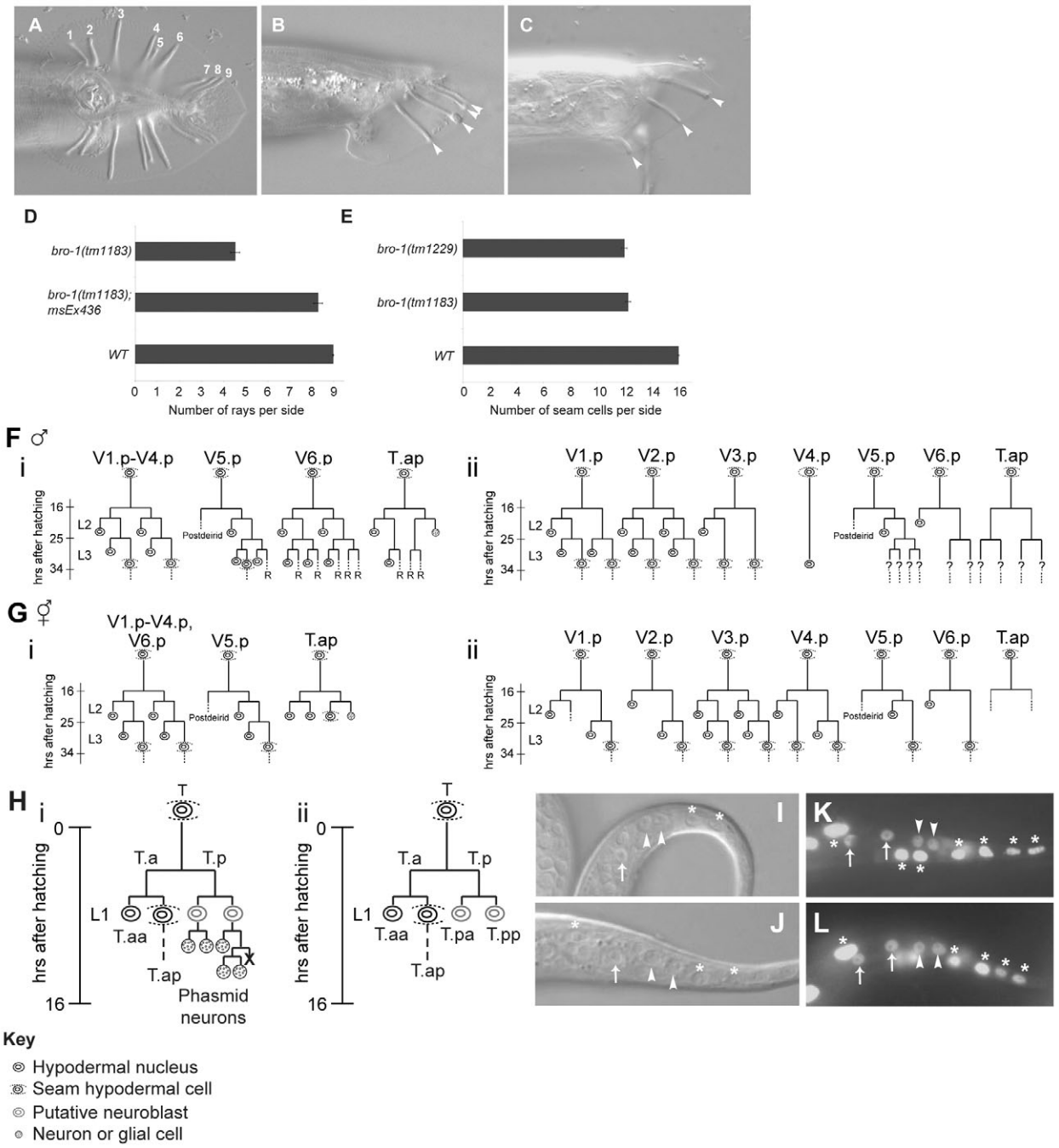

Fig. 2. Loss of *bro-1* function causes V- and T-lineage-specific division failures, resulting in ray loss. (**A**) *him-8(e1489)* male tail, with the characteristic nine rays per side (numbered). (**B**) *rnt-1(ok351); him-8(e1489)* male tail. Arrowheads indicate four rays visible on the left side. (**C**) *bro-1(tm1183); him-8(e1489)* male tail. Arrowheads indicate three visible rays. (**D**) Bar chart showing ray number in *him-8(e1489)* (*n*=102; effectively WT), *bro-1(tm1183); him-8(e1489)* (*n*=94) and *bro-1(tm1183); him-8(e1489); msEx436[pHK196 + rol-6]* (*n*=43) males. Error bars represent the standard error of the mean (s.e.m.). (**E**) Bar chart showing seam cell number in WT adult hermaphrodites carrying the seam cell marker *SCM::GFP* (strain JR667; *n*=70), *bro-1(tm1183); SCM::GFP* (*n*=83) and *bro-1(tm1229); SCM::GFP* (*n*=54) hermaphrodites. (**F**,**G**) Lineage trace of V1-V6 and T divisions in WT and *bro-1* animals up to mid L3. The L1 asymmetric division is omitted for simplicity. Broken lines indicate incomplete lineages. Question mark indicates fate was not determined. The data shown are lineage traces for single animals but are representative of several lineaged animals. (Fi) WT male. (Gi) WT hermaphrodite. Divisions are as previously described (Sulston et al., 1980). F(ii): *bro-1(tm1183)* male. Several division failures are evident as shown. (Gii) *bro-1(tm1183)* hermaphrodite. A similar scale of defects is observed. (**H**) Lineage trace of the T divisions in WT and *bro-1* animals during L1. (Hi) WT hermaphrodite. (Hii) *bro-1(tm1183)* hermaphrodite. The anterior branch of the T lineage looks normal, but the posterior branch fails. T.pa and T.pp have a hypodermal appearance and fail to divide further. (**I-L**) Nomarski and fluorescence (*dpy-7::GFP*) images of T-lineage cells in WT and *bro-1* L1 animals. Asterisks indicate hypodermal nuclei. White arrowheads indicate T.px nuclei T.pa and T.pp and white arrows indicate T.ax hypodermal/seam nuclei. (I) WT L1 hermaphrodite. (J) *bro-1(tm1183)* L1 hermaphrodite. T.px nuclei look hypodermal in both strains. (K) WT L1 hermaphrodite carrying *dpy-7::GFP*. (L) *bro-1(tm1183)* L1 hermaphrodite carrying *dpy-7::GFP* (strain AW194). *dpy-7::GFP* expression is similar in all four nuclei in both strains.

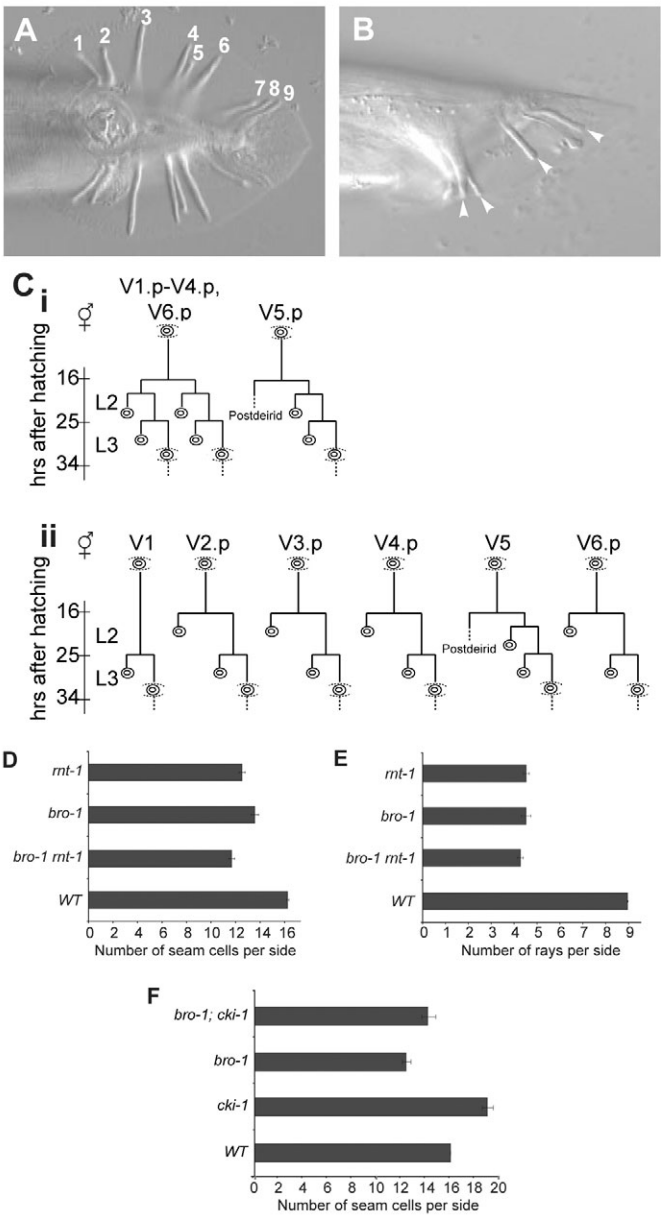

Fig. 3. *bro-1 rnt-1* double mutants have a similar phenotype to single mutants. (**A**) *him-8(e1489)* male tail. (**B**) *bro-1(tm1183) rnt-1(tm388); him-5(e1490)* male tail. White arrowheads indicate four rays visible in this animal. (**C**) V lineage traces up to mid L3, omitting the L1 asymmetric division. The symbols used for different cell types are the same as for Fig. 2. (Ci) WT hermaphrodite. (Cii) *bro-1(tm1183) rnt-1(tm388)* hermaphrodite. (**D**) Bar chart showing seam cell number in *him-5(e1490)* hermaphrodites carrying *SCM::GFP* (strain AW60; *n*=24; effectively WT), *bro-1(tm1183); him-5(e1490) SCM::GFP* hermaphrodites (strain AW186; *n*=37), *rnt-1(tm388); him-5(e1490) SCM::GFP* hermaphrodites (strain AW187; *n*=53) and *bro-1(tm1183) rnt-1(tm388); him-5(e1490) SCM::GFP* hermaphrodites (strain AW180; *n*=47). (**E**) Bar chart showing ray number in *him-8(e1489)* males (*n*=102), *bro-1(tm1183); him-8(e1489)* males (*n*=94), *rnt-1(tm388); him-8(e1489)* males (*n*=84) and *bro-1(tm1183) rnt-1(tm388); him-8(e1489)* males (*n*=97). (**F**) Bar chart showing seam cell number in the adult hermaphrodite progeny of *him-5(e1490)* and *bro-1(tm1183); him-5(e1490)* mutant animals that had been either subjected to RNAi of the *cki-1* gene (*cki-1*, *n*=23; *bro-1; cki-1*, *n*=24) or injected with TE only as a control (*WT*, *n*=21; *bro-1*, *n*=21).

is the case for either single mutant. In addition, double mutants also have a slightly lower number of seam cells on average. This suggests that there may be aspects of the functions of RNT-1 and BRO-1 that are distinguishable from one another, even though the major functions of RNT-1 and BRO-1 in controlling seam cell lineage development are co-dependent.

Previously, we have shown that seam cell expression of the cyclin-dependent kinase inhibitor *cki-1* is up-regulated in *rnt-1* mutants, and that *cki-1* RNAi partially restores seam cell number in *rnt-1* mutants (Nimmo et al., 2005). To test whether *cki-1* is also a likely downstream target of BRO-1, we performed *cki-1* RNAi in a *bro-1* mutant background (Fig. 3F). *bro-1; cki-1(RNAi)* animals were found to have more seam cells than *bro-1* mutants alone, with numbers restored almost to WT levels, similar to data previously published for *rnt-1*. This suggests that RNT-1 and BRO-1 act in a common pathway to repress *cki-1* expression in seam cells during key stages of larval development.

bro-1 is co-expressed with *rnt-1* in seam and muscle cells, and additionally expressed in the uterine seam

The expression pattern of *bro-1* in transgenic animals containing a full-length rescuing *bro-1::GFP* reporter (pHK193) is shown in Fig. 4. Similar expression patterns were observed for a variety of different transgenic alleles, carrying both extrachromosomal and integrated arrays (data not shown). In all larval stages, BRO-1::GFP is expressed in H0-2, V1-6 and T seam progeny. BRO-1::GFP is localised to both the cytoplasm and nucleus, similar to the expression pattern reported for CBFβ in mammalian cells (Tanaka et al., 1997). It seems probable, therefore, that the sub-cellular localisation of CBFβ is conserved. We cannot exclude the possibility, however, that cytoplasmic localisation results from the presence of a GFP fusion, or from overexpression. Faint expression is also observed in hypodermal nuclei, some of which are embryonically derived and which are not therefore simply anterior daughters of the L1 stem cell division containing a perdurance of GFP expression. We also observed expression of BRO-1::GFP in the uterine seam (utse) during late L4 in hermaphrodites (Fig. 4B). This expression is likely to be due to diffusion of cytoplasmic BRO-1::GFP as a result of fusion of the utse with the seam in L4, but also raises the possibility that BRO-1 has a functional role in this tissue.

Intriguingly, we noticed that *bro-1::GFP* animals contain extra seam cells. For example, an L3 *bro-1::GFP*-expressing animal is shown in which V1-derived seam cells have over-proliferated (Fig. 4C). In this animal, the anterior progeny of the V1.pa and V1.pp L2 stem cell divisions have not fused with the hypodermal syncytium but instead have remained as seam and undergone further division in L3, giving rise to eight nuclei instead of the expected four.

The expression pattern of BRO-1 in seam cells is very similar to that of RNT-1 (except that RNT-1::GFP is always nuclear), and co-localisation is shown using rescuing *bro-1::DsRed* (pAW303) and *rnt-1::GFP* (pAW260) constructs (Fig. 4D). Co-localisation is consistent with the hypothesis that BRO-1 acts together with RNT-1 to control seam cell divisions. Faint BRO-1::RFP and RNT-1::GFP co-localisation is also observed in certain body wall muscle cells (Fig. 4E). Muscle expression of RNT-1 has been previously reported although no functional role has been described (Kagoshima et al., 2005; Nimmo et al., 2005). Finally, we also observed BRO-1::RFP, but not RNT-1::GFP, in certain pharyngeal neurons. In short, BRO-1 and RNT-1 are co-expressed in seam and muscle cells, and BRO-1 is additionally expressed in hypodermal nuclei, certain pharyngeal neurons and the utse.

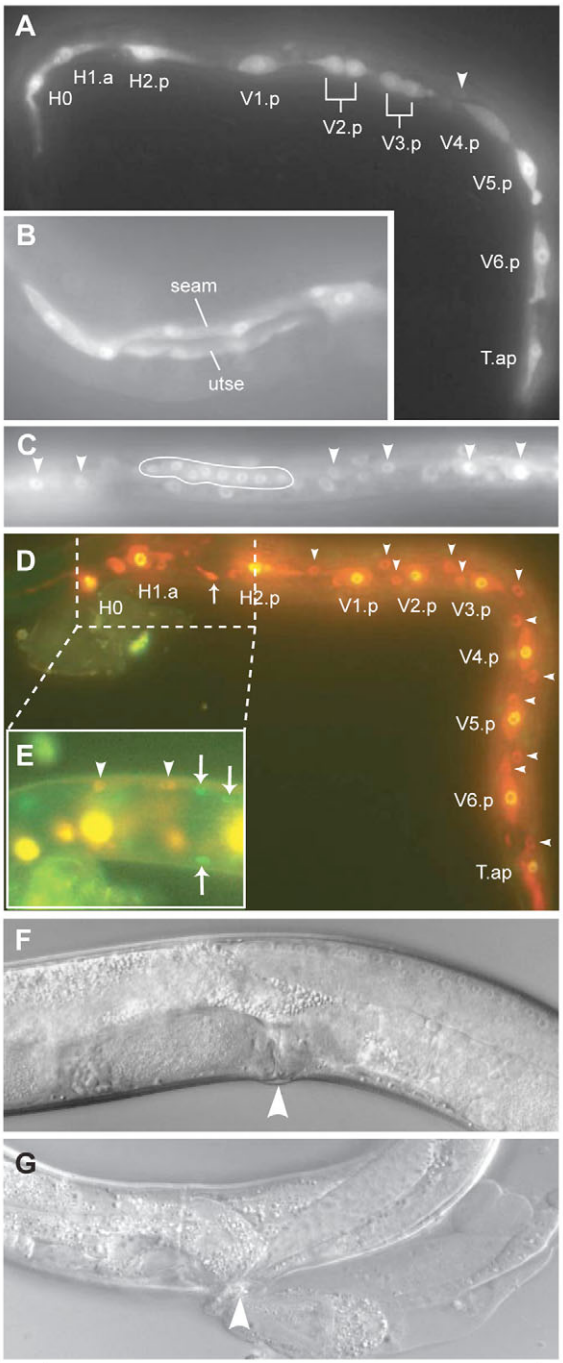

H

Genotype	Rup	Pvl	Bag	WT	Total	% Vulva Abnormal
N2	0	0	0	100	100	0%
rnt-1	2	0	0	94	96	2%
bro-1	15	1	1	69	86	20%
bro-1 rnt-1	27	3	5	61	96	37%

Fig. 4. BRO-1 and RNT-1 are largely co-expressed. (**A-C**) Animals carrying an integrated *bro-1::GFP* reporter construct (*dpy-20 (e2017)IV*; *msIs344[pHK196 bro-1::GFP + pMH86])* (strain YK149). (A) Larva around the L1-L2 molt. Most seam cells (labelled) are undivided in this animal except V2.p and V3.p. Faint expression is also observed in some hyp7 nuclei (white arrowhead). (B) BRO-1::GFP in the seam and uterine seam (utse) in adult hermaphrodite, after fusion of these compartments in L4. (C) L3 larva in which V1.p-derived seam cells have over-proliferated (extra nuclei are indicated by the white oval outline). Seam cells yet to divide are indicated by white arrowheads. Faint hyp7 expression is again observed in nuclei of both embryonic and larval origin (all unlabelled nuclei). (**D**) WT larva around the L1-L2 molt carrying both *bro-1::DsRed* and *rnt-1::GFP* translational reporter constructs (strain AW192, *ouEx43*). Co-expression can be clearly observed in all 10 seam cell nuclei, which have yet to divide in L2 (labelled, fluorescence appears yellow). BRO-1::RFP, but not RNT-1::GFP expression, is also observed in hypodermal nuclei (white arrowheads) and certain pharyngeal neurons (white arrow). (**E**) Higher magnification image (×1.33) of a different focal plane of region of specimen in D showing co-localisation of BRO-1::RFP and RNT-1::GFP in certain body wall muscle nuclei (white arrowheads). Other body wall muscle nuclei look green, and are therefore expressing *rnt-1* only (white arrows). (**F**) WT young adult showing fully formed vulva (white arrowhead). (**G**) *bro-1(tm1183) rnt-1(tm388)* adult hermaphrodite that has ruptured at the vulva at the L4-adult molt (white arrowhead). (**H**) Table showing penetrance of vulval defects in N2 WT, *rnt-1(tm388)*, *bro-1(tm1183)* and *bro-1(tm1183) rnt-1(tm388)* hermaphrodites. Rup, ruptured vulva; Pvl, protruding vulva; Bag, 'bag of worms' phenotype due to hatching of eggs inside mother.

bro-1-specific phenotypes

Closer examination of *bro-1* mutant hermaphrodites revealed rupturing at the vulva and eversion of the gonad at the L4 molt in around 20% of hermaphrodites (Fig. 4G,H), suggesting a possible defect in either the uterine-vulval or uterine-hypodermal connection. The penetrance of this phenotype is almost doubled in *bro-1(tm1183) rnt-1(tm388)* double mutants, but is observed only occasionally in *rnt-1* single mutants (Fig. 4H). The origin of the vulval defect is not clear at present. We could see no obvious defects in *bro-1rnt-1* double mutants using a variety of markers, including *egl-13::GFP* and *cdh-3::GFP* reporters to observe the arrangement of the utse, and utse-seam cell fusion, respectively (Cinar et al., 2003; Pettitt et al., 1996) (data not shown). It is possible that the reduced number of nuclei in the seam and/or hypodermal syncytium in the vicinity of the vulva in *bro-1* and *bro-1 rnt-1* mutants, somehow acts to weaken the uterine-hypodermal connection. However, the observed expression of BRO-1 in the utse together with the much higher penetrance of vulval and/or uterine defects in *bro-1* compared with *rnt-1* animals, suggests that BRO-1 may have a specific role in vulval and/or uterine morphogenesis that is, at least in part, independent of RNT-1.

BRO-1 interacts directly with RNT-1, acting to increase the affinity and specificity of RNT-1/DNA interactions

We used electophoretic mobility shift assays (EMSAs) to investigate BRO-1-RNT-1 interaction. The GST-tagged Runt domain of RNT-1 (GST-RD) binds weakly to the consensus Runx DNA binding site AACCGCA (Fig. 5A). However, this interaction lacks specificity, as a mutated competitor probe reduces the band shift as effectively as WT competitor (Fig. 5A). The addition of BRO-1 protein stimulates both the affinity of RNT-1 for the DNA binding consensus, and the

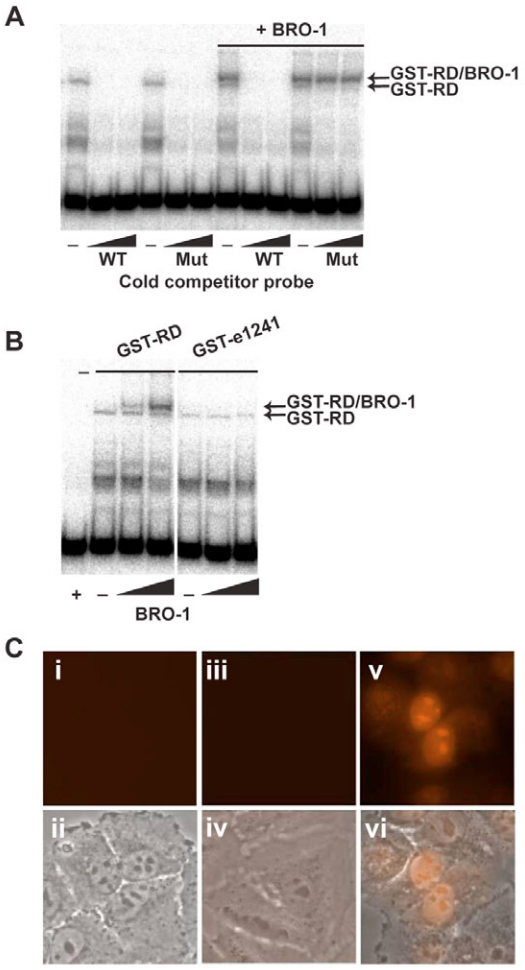

Fig. 5. Biochemical analysis of BRO-1-RNT-1 interaction. (**A**) EMSA showing BRO-1-RNT-1 interaction. Lanes 1 and 4: GST-RNT-1 Runt domain (GST-RD) purified protein (20 ng) incubated with Runx consensus DNA binding site probe AACCGCA (10 fmol). A weak band shift can be observed (arrow) that is abolished by the addition of 30× (300 fmol); lane 2) or 100× (1 pmol; lane 3) of cold WT competitor. However, a mutated version of the competitor probe (AATCGAA), at 30× (lane 5) or 100× (lane 6), is also able to abolish RNT-1-DNA binding. The addition of purified BRO-1 protein (100 ng) to the reaction (lanes 7 and 10) causes the GST-RD band to be super-shifted and enhanced. These band shifts are still abolished by a cold WT competitor probe at 30× (lane 8) or 100× (lane 9), but this time the mutated competitor probe, added at 30× (lane 11) or 100× (lane 12), is unable to diminish RNT-1-DNA binding. (**B**) EMSA showing the RNT-1 *e1241* point mutant $I_{112}K$ does not interact with BRO-1. Lane 1, Runx consensus DNA binding site probe incubated with purified BRO-1 (1000 ng). No band shift is observed indicating that no non-specific DNA binding is occurring. Lane 2, 20 ng WT GST-RD incubated with Runx probe showing same band shift as in A. Increasing amounts of BRO-1 (lanes 3 and 4, 10 ng and 100 ng, respectively) causes the RNT-1-DNA band shift to be supershifted and enhanced as expected. Lane 5, 40 ng of GST-e1241 (Runt domain of RNT-1 containing the $I_{112}K$ mutation found in the *e1241 rnt-1* allele) incubated with Runx probe. Incubation with increasing amounts of BRO-1 (lanes 6 and 7, 10 ng and 100 ng, respectively) has no effect on the band shift, indicating that $I_{112}K$ RNT-1 does not interact with BRO-1. (**C**) RUBY experiment showing direct interaction between BRO-1 and RNT-1 in mammalian cells. (i,iii,v) Fluorescence images. (ii,iv,vi) Merged fluorescence and phase contrast images. (i,ii) Cells expressing a RUBY-BRO-1 fusion. (iii,iv) Cells expressing a monomeric RUBY-RNT-1RD (Runt domain of RNT-1) fusion. (v,vi) Cells co-expressing both RUBY-BRO-1 and RUBY-RNT-1RD fusions.

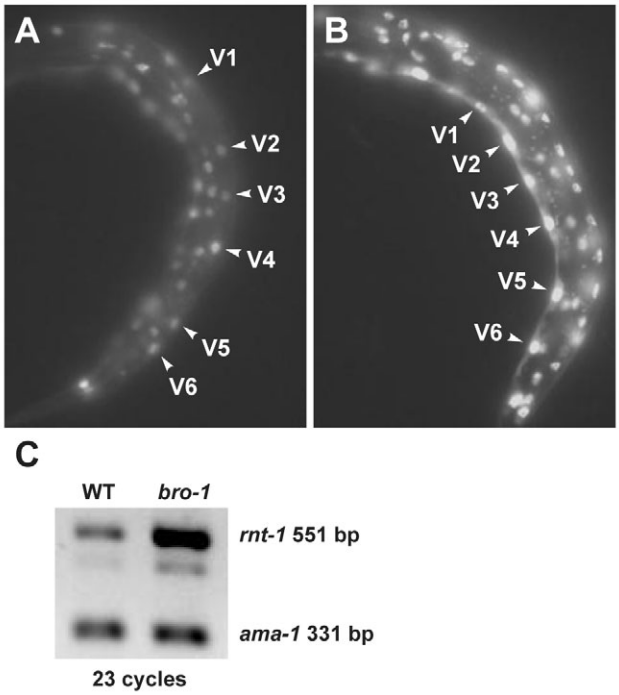

Fig. 6. BRO-1 represses *rnt-1* expression. (**A**) *rnt-1::GFP* expression (*msIs114[pHK192 + rol-6]*) in a *bro-1(tm1183)* L1 larva rescued with *bro-1::RFP* (*msEx446[pHK328]*) (strain YK153). (**B**) L1 larva of the same strain, but this animal has lost the *bro-1::RFP* rescuing array. Both images were taken under identical exposure conditions. It was not possible to observe adult hermaphrodites carrying a *rnt-1::GFP* transgene and *bro-1(tm1183)* mutation because these animals invariably die during late larval development as a result of rupture of the vulva. Hence the strain used in these experiments consisted of an integrated *rnt-1::GFP* transgene in a *bro-1(tm1183)* mutant background kept alive by extrachromosomal rescuing *bro-1::RFP*. (**C**) RT-PCR analysis of *rnt-1* transcripts in WT and *bro-1(tm1183)* animals. *ama-1* is an internal control. The smaller, fainter band is an alternatively spliced variant of *rnt-1* (T. Braun and A.W., unpublished).

specificity of the interaction, as mutated competitor probe fails to reduce the RNT-1-DNA shift in the presence of BRO-1 (Fig. 5A). Next we tested the *rnt-1(e1241)* mutant protein RNT-1 Runt domain $I_{112}K$ (substitution of Lys for Ile_{112}). The I_{112} residue of RNT-1 is equivalent to V_{152} of murine Runx1, which is located within the exposed β sheet region of Runx1, known as β10, situated at the Runx1-CBFβ heterodimerisation interface (Tahirov et al., 2001). However, alanine scanning mutagenesis experiments have suggested a role for V_{152} in DNA binding, rather than CBFβ interaction (Li et al., 2003). By contrast, the data in Fig. 5B shows that RNT-1 $I_{112}K$ fusion protein (GST-e1241) retains weak DNA binding activity but does not supershift upon addition of BRO-1, indicating that I_{112} is required for heterodimer formation and therefore high affinity DNA binding.

To confirm that BRO-1 and RNT-1 interact directly, we used the RUBY system. This assay is based on the fact that monomeric DsRed1 is subject to conditional proteolysis and rapid degradation through the ubiquitin-proteasome pathway, but escapes degradation in the associated, dimeric state. Interaction of the proteins of interest brings the linked DsRed1 monomers into close proximity and enables their dimerisation and maturation (J. Tanaka and Y.M., unpublished). The data in Fig. 5C

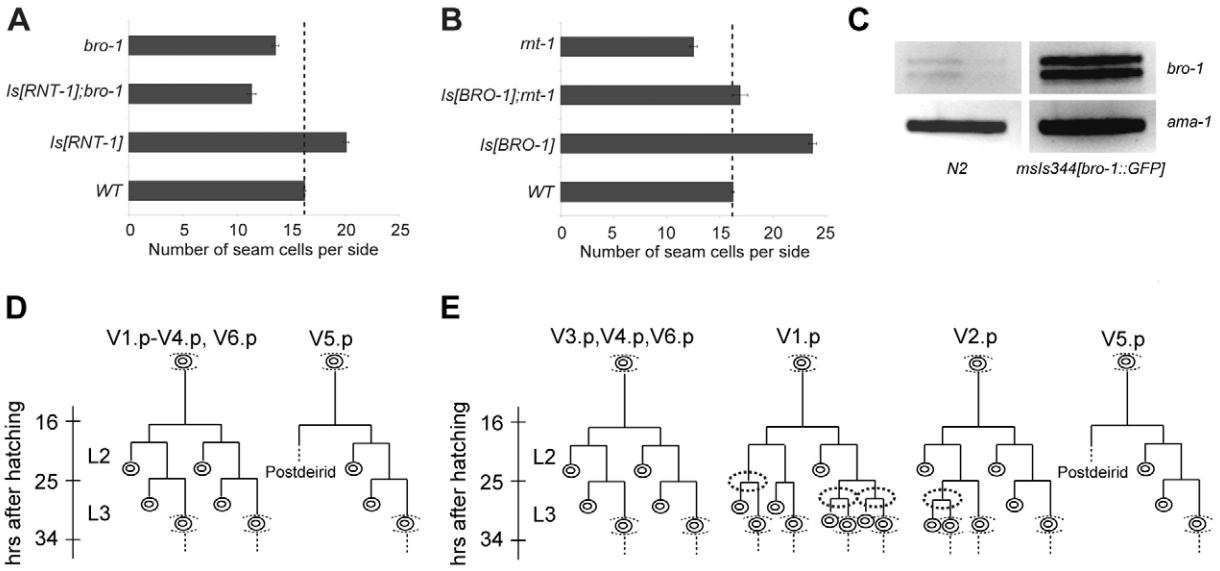

Fig. 7. BRO-1- and RNT-1-induced seam cell hyperplasia. (**A**) Bar chart showing seam cell number in *him-5(e1490) SCM::GFP* L4 hermaphrodites (strain AW60; *n*=24) (effectively WT), and animals with the same reporter carrying an integrated *rnt-1::GFP* transgene (*msIs114*, labelled as *Is[RNT-1]*, strain AW189; *n*=55), an integrated *rnt-1::GFP* transgene in a *bro-1(tm1183)* mutant background (strain AW191; *n*=23), and those with a *bro-1(tm1183)* mutation alone (strain AW186; *n*=37). The dotted line represents WT seam cell number (16 per side). As strains containing the integrated *rnt-1::GFP* transgene in a *bro-1* mutant background tend to die around the L4-adult transition it was necessary to keep strain AW191 viable using an extrachromosomal rescuing *bro-1::RFP* array. Seam cell number was then counted in animals that had lost the array. (**B**) Bar chart showing seam cell number in *SCM::GFP him-5(e1490)* L4 hermaphrodites (*n*=24; effectively WT), and animals with the same reporter carrying an integrated *bro-1::GFP* transgene, *msIs344* (labelled as *Is[BRO-1]*, strain AW188; *n*=57), an integrated *bro-1::GFP* transgene in a *rnt-1(tm388)* mutant background (strain AW185; *n*=41), and those with a *rnt-1 (tm388)* mutation alone (strain AW187; *n*=53). (**C**) Expression level of *bro-1* mRNA in WT and *msIs344[bro-1::GFP]* strains, measured using semi-quantitative RT-PCR. The doublet seen for *bro-1* corresponds to the full length *bro-1* transcript and a shorter alternatively spliced form. (**D**,**E**) Lineage analysis of BRO-1-induced seam cell hyperplasia. V lineage traces are shown up to mid L3, omitting the L1 asymmetric division. (D) WT hermaphrodite. (E) Hermaphrodite overexpressing *bro-1* (by carrying an integrated *bro-1::GFP* array, *msIs344*, strain YK149). Extra divisions were observed in V1.p and V2.p. In V1.p, the division of the anterior seam daughter of the symmetrical division at the beginning of L2 is itself symmetrical, giving rise to an anterior daughter that retains seam (stem-cell) characteristics rather than adopting the hypodermal fate. This extra seam cell then divides asymmetrically along with the other seam cells in L3 (circled with a dashed line). In the posterior branch there is an extra proliferative (symmetrical) division at the beginning of L3, giving rise to two seam daughters capable of further (asymmetric) division (circled with a dashed line). In V2.p, the division of the anterior V2-derived seam cell is transformed into a symmetrical division, giving rise to an anterior daughter that retains seam (stem-cell) characteristics (circled with a dashed line), and quickly divides further. Overall, three extra seam cells have been produced by these lineage alterations during L2 and early L3.

show fluorescence output from cells expressing either RUBY-BRO-1 or RUBY-RNT-1RD fusions (RD: Runt domain of RNT-1), and from cells co-expressing both fusions. A strong fluorescence signal is only visible when BRO-1 and RNT-1 are co-expressed, indicating that the two proteins form a heterodimer. Neither protein appears to homodimerise. Positive and negative controls for this technique, using Runx2 and CBFβ RUBY fusions, can be seen in Fig. S1 (see Fig. S1 in the supplementary material).

RNT-1 is upregulated in *bro-1* mutants

In order to test for possible regulatory interactions between RNT-1 and BRO-1, we examined BRO-1 expression in *rnt-1* mutants, and vice versa. The absence of RNT-1 had no effect on either the pattern or level of BRO-1::GFP expression (data not shown). In the converse experiment, however, we observed upregulation of RNT-1::GFP in *bro-1* mutant L1 larvae in both seam and muscle cells (Fig. 6B). This result was surprising as in mammalian cells CBFβ acts in the opposite way, stabilising Runx proteins by preventing their ubiquitination (Huang et al., 2001). To investigate whether this negative regulation of RNT-1 by BRO-1 was occurring at the level of transcription we analysed animals by RT-PCR and found a corresponding increase in *rnt-1* mRNA in *bro-1* mutant larvae compared with WT (Fig. 6C). Therefore BRO-1 acts, either directly or indirectly, as a transcriptional repressor of *rnt-1*.

Overexpression of *bro-1* causes seam cell hyperplasia

Previously we reported that overexpression of *rnt-1* cDNA from the heat shock promoter at particular stages of development causes an increase in the number of seam cells (Nimmo et al., 2005). We have repeated these experiments using constitutive overexpression of *rnt-1* from the integrated *rnt-1::GFP* rescuing transgenic strain *msIs114* and find that this strain also contains extra seam cells (Fig. 7A) due to overexpression of *rnt-1* from multiple copies of the gene in transgenic arrays (data not shown). Extra seam cells were observable in a variety of different *rnt-1* transgenic strains, containing independent arrays and constructs (data not shown). We therefore also tested constitutive *bro-1* overexpression using the integrated rescuing *bro-1::GFP* strain *msIs344* (expressing high levels of *bro-1* mRNA as shown in Fig. 7C) and found that this too causes seam cell hyperplasia (Fig. 7B, also discussed earlier, see Fig. 4C). Likewise, extra seam cells could be seen in a variety of different *bro-1* multicopy transgenics (data not shown).

BRO-1-induced hyperplasia is RNT-1 independent

We found that overexpression of RNT-1 in *bro-1* mutants does not compensate for the reduction in seam cell number (Fig. 7A). In fact, the number of seam cells is slightly lower in *rnt-1::GFP bro-1(tm1183)* animals compared with *bro-1* mutant animals alone. Perhaps RNT-1 has a dominant-negative effect in the absence of BRO-1, possibly by binding to non-specific sites in DNA (as suggested by our EMSA data) and recruiting, and therefore titrating, other transcriptional co-factors away from RNT-1 target sites.

However, the converse experiment, in which BRO-1 was overexpressed in a *rnt-1* mutant background (the *tm388 rnt-1* allele used is a presumed null), did give rise to animals with extra seam cells (Fig. 7B), suggesting that BRO-1 can function to promote seam cell divisions independently of RNT-1 activity. This, taken together with data showing vulval roles for BRO-1 that are, at least in part, independent of RNT-1, is strongly suggestive of the RNT-1-independent nature of various aspects of BRO-1 function. RNT-1-independent roles for BRO-1 are unprecedented as previous data from other systems always considers Runx/CBFβ solely as a co-dependent DNA binding complex.

Cellular basis of seam cell hyperplasia

Seam cell hyperplasia could be caused either by an increased number of seam cell divisions (increased self-renewal and proliferation) or by changes in fate resulting from a loss of asymmetry. The lineage data shown in Fig. 7C indicate that transgenic animals overexpressing *bro-1* do indeed go through extra, unscheduled seam cell divisions but in addition, some of the L2 and L3 asymmetrical stem cell divisions are now transformed to symmetrical divisions resulting in increased self-renewal. The anterior progeny of these stem cell divisions are prevented from acquiring the hypodermal fate and fail to fuse with the hypodermal syncytium. This is a fate change, although in this case the 'fate' is to retain the seam characteristic of continued proliferation, giving rise to an extra stem cell division and thus an extra seam cell. In this way BRO-1 (acting, at least partly, together with RNT-1) functions to promote the stem-like (self-renewal) characteristics of seam cell divisions at the expense of the acquisition of the differentiated, hypodermal fate.

Co-overexpression of *bro-1* and *rnt-1* causes seam cell 'tumours'

We also counted seam cell number in a strain containing both *rnt-1* and *bro-1* integrated arrays. The co-overexpression of RNT-1 and BRO-1 produces massive seam cell hyperplasia, 49 cells on average per side (and up to 70) instead of the 16 expected in WT (Fig. 8A). This extreme seam cell hyperplasia causes lateral expansion of the seam (Fig. 8C,D) and animals containing these seam cell 'tumours' are fatter (although shorter) than WT (Fig. 8E,F).

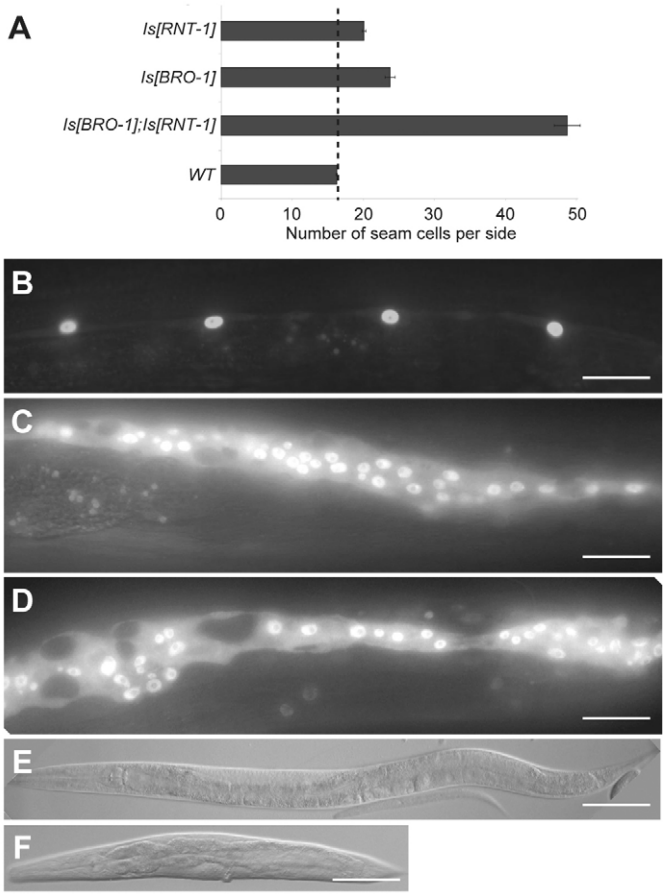

Fig. 8. Co-overexpression of *bro-1* and *rnt-1* induces massive seam cell hyperplasia. (**A**) Bar chart showing seam cell number in *SCM::GFP him-5(e1490)* L4 hermaphrodites (*n*=24; effectively WT), and animals with the same reporter carrying an integrated *bro-1::GFP* transgene (labelled as *Is[BRO-1]*, strain AW188; *n*=57), an integrated *rnt-1::GFP* transgene (labelled as *Is[RNT-1]*, strain AW189; *n*=55), and both integrated *bro-1::GFP* and *rnt-1::GFP* transgenes (labelled as *Is[BRO-1];Is[RNT-1]*, strain AW190; *n*=38). (**B**) Seam cell nuclei along the mid body region of a WT L4 hermaphrodite animal carrying the *SCM::GFP* reporter. Scale bar: 25 μm. (**C**,**D**) Similar region of L4 hermaphrodites co-overexpressing *bro-1::GFP* and *rnt-1::GFP* as well as *SCM::GFP* (strain AW190). Scale bars: 25 μm. (**E**,**F**) Low power images showing whole worms. Scale bars: 100 μm. (E) WT adult hermaphrodite. (F) Adult hermaphrodite co-overexpressing *bro-1::GFP* and *rnt-1::GFP*.

DISCUSSION

BRO-1 is a CBFβ homologue and acts to control seam cell number

Despite the relatively low level of sequence homology between BRO-1 and CBFβ, we have presented strong genetic and biochemical evidence that BRO-1 is a binding partner for RNT-1, and acts in concert with RNT-1 to regulate seam cell number. Our lineage analysis demonstrates that the ray loss phenotype seen in *bro-1* alleles is caused by failed cell divisions in seam lineages, and is very similar to that reported previously for *rnt-1* mutants (Nimmo et al., 2005). *bro-1 rnt-1* double mutants have similar rates of ray loss to either single mutant, suggesting that a major role of these two genes is to act in a common pathway to promote seam cell proliferation and/or self-renewal, with *cki-1* as a probable direct or indirect downstream target.

BRO-1 increases both the affinity and specificity of RNT-1-DNA interactions

BRO-1 and RNT-1 are both expressed in seam cells, consistent with the hypothesis that they act in concert to regulate seam cell divisions. The RUBY assay indicates a direct interaction between BRO-1 and RNT-1 and EMSA studies demonstrate that BRO-1 is required for robust binding of RNT-1 to the Runx consensus DNA binding site, consistent with other studies of CBFβ function (Bushweller, 2000; Li et al., 2003; Nagata and Werner, 2001; Tahirov et al., 2001; Yan et al., 2004). Furthermore, our experiments show that BRO-1

dramatically increases the specificity of RNT-1-DNA binding, thereby extending previous studies of CBFβ/Runx interactions. It will be of interest to investigate whether this finding can be extended to other systems.

BRO-1 displays some RNT-1-independent activity

BRO-1, as well as RNT-1, promotes extra seam cell divisions when overexpressed, acting to promote self-renewal. Intriguingly, BRO-1 is capable of promoting extra divisions in the absence of RNT-1, thus suggesting that BRO-1 has Runx-independent functionality, an observation confirmed by the enhanced vulval rupture of *bro-1* mutants compared to *rnt-1* mutants. The converse is not true: RNT-1 is only capable of promoting extra divisions in the presence of functional BRO-1, perhaps because of the importance of BRO-1 in influencing the specificity and robustness of RNT-1-DNA interactions. Likewise, the late larval lethality of the *rnt-1::GFP* transgene in a *bro-1* mutant background (see legend to Fig. 6) may be related to the role we have demonstrated for BRO-1 in increasing the specificity of RNT-1-DNA interactions. In the absence of BRO-1, RNT-1 (already overproduced in a transgenic animal) may bind promiscuously to ectopic sites, thus misregulating gene expression and impairing transcriptional networks.

Our finding that BRO-1 does not appear to be wholly reliant on RNT-1 in order to promote seam cell proliferation is the first indication that CBFβ proteins in general may have Runx-independent functions. Perhaps RNT-1 and BRO-1 regulate transcription as part of the core of a large enhanceosome or repressosome complex, as proposed for the mammalian Runx factors (Carey, 1998), and BRO-1 is able to interact, albeit less efficiently, with this complex even in the absence of RNT-1. Alternatively it may have some other intrinsic activity associated with the control of seam cell proliferation and/or self-renewal.

BRO-1 and RNT-1 co-overexpression causes seam 'tumours'

Co-overexpression of RNT-1 and BRO-1 causes massive hyperproliferation of seam cells, supporting the view that the major function of RNT-1 and BRO-1 is to co-operate as a complex in the transcriptional regulation of genes required to control seam cell number. The resulting hyperplasia distorts the morphology and integrity of the seam, causing it to expand dorsoventrally and invade the surrounding syncytial hypodermis, resulting in fatter but shorter (Dumpy) animals. *C. elegans* do not exhibit solid somatic tumours as such. The germline is the one other well-established 'tumour' system, where failure of mitotic germ nuclei to enter meiosis, caused for example by gain of *glp-1* function (Berry et al., 1997; Crittenden et al., 2003), can result in massive mitotic over-proliferation and a concomitant expansion of the gonad. We hypothesise that because of the restriction on body volume exerted by the cuticle, expansion in one direction probably leads to contraction in the other, hence, worms with much increased numbers of seam nuclei resulting form the overexpression of both *bro-1* and *rnt-1* are shorter and fatter because of lateral expansion, whereas worms with increased syncytial hypodermal ploidy are known to be longer than WT (Flemming et al., 2000), i.e. to expand longitudinally. Perhaps this extreme hyperplasia is as close to a somatic 'tumour' that this model organism can get.

One way in which the levels of these genes may be controlled is via negative feedback, and indeed we have discovered that loss of *bro-1* is associated with increased expression of *rnt-1*. BRO-1 may either be acting in a RNT-1-independent manner to repress *rnt-1* expression, or as part of a *rnt-1* autoregulatory feedback loop. It is presumably necessary to limit the amount of functional Runx/CBFβ complexes in order to program the correct cell division pattern of the seam lineage.

Conservation of BRO-1-RNT-1 function

There are numerous reports in the literature of Runx genes and *CBFβ* acting either as proto-oncogenes or tumour suppressors, the nature of which is highly context dependent (Blyth et al., 2005; Cameron and Neil, 2004). It is not clear whether such roles in carcinogenesis arise as a result of defects in cellular differentiation or cell proliferation. The analysis of cell proliferation at the single cell level, which is the hallmark of *C. elegans* studies, leads us to conclude that BRO-1 and RNT-1 act to promote the self-renewal characteristics of seam stem cell divisions at the expense of the differentiated, hypodermal fate. Thus, our studies would support the view that Runx/CBFβ factors have oncogenic potential.

Rationalising the, sometimes contradictory, effects of Runx/CBFβ factors on cellular development, especially in carcinogenesis, is one of the toughest challenges in understanding the function of these important genes. We have now firmly established *C. elegans* as a prominent model organism for the study of Runx/CBFβ function, as we can interpret phenotypes in individual cells rather than being forced to rely on analyses of cell populations and tissues, and can work without the interpretative difficulties caused by genetic redundancy that are inherent in other experimental systems where there are multiple Runx genes. One of the interesting ideas to emerge from these studies is that it may not be appropriate to regard BRO-1 simply as a partner subunit for high affinity RNT-1-DNA binding. Although a major role of BRO-1 is to cooperate with RNT-1 to promote seam cell proliferation and/or self-renewal (presumably by stabilising RNT-1-DNA interactions) BRO-1 also increases the specificity of RNT-1-DNA interactions, has a role in the transcriptional regulation of *rnt-1*, and furthermore appears to have functions in the worm that are, at least in part, independent of RNT-1. It will be of interest to see whether our findings can be extended to other systems.

We thank J. Kajiwara for excellent technical help, K. Shigesada for critical reading of the manuscript, A. Fire, R. Tsein and H. Tabara for vectors and plasmids, and members of the Kohara and Woollard laboratories for comments and discussion on the manuscript. We would also like to thank the CGC and I. Johnstone for strains. Work in Y.K.'s laboratory was supported by a Grant-in-Aid for Scientific Research on Priority Areas from the Ministry of Education, Culture, Sports, Science and Technology of Japan. Work in A.W.'s laboratory was funded by the UK Medical Research Council, the Association for International Cancer Research and Cancer Research-UK. Work in Y.M.'s laboratory was supported by Grant-in-Aid for Scientific Research on priority areas 'System Genomics (18016002)', 'Nuclear Dynamics (17050004)' and 'G-protein signal (18057003)'.

Supplementary material

Supplementary material for this article is available at
http://dev.biologists.org/cgi/content/full/134/21/3905/DC1

References

Adya, N., Stacy, T., Speck, N. A. and Liu, P. P. (1998). The leukemic protein core binding factor beta (CBFbeta)-smooth-muscle myosin heavy chain sequesters CBFalpha2 into cytoskeletal filaments and aggregates. *Mol. Cell. Biol.* **18**, 7432-7443.

Adya, N., Castilla, L. H. and Liu, P. P. (2000). Function of CBFbeta/Bro proteins. *Semin. Cell Dev. Biol.* **11**, 361-368.

Berry, L. W., Westlund, B. and Schedl, T. (1997). Germ-line tumor formation caused by activation of glp-1, a *Caenorhabditis elegans* member of the Notch family of receptors. *Development* **124**, 925-936.

Blyth, K., Cameron, E. R. and Neil, J. C. (2005). The RUNX genes: gain or loss of function in cancer. *Nat. Rev. Cancer* **5**, 376-387.

Bushweller, J. H. (2000). CBF – a biophysical perspective. *Semin. Cell Dev. Biol.* **11**, 377-382.
Cameron, E. R. and Neil, J. C. (2004). The Runx genes: lineage-specific oncogenes and tumor suppressors. *Oncogene* **23**, 4308-4314.
Canon, J. and Banerjee, U. (2003). In vivo analysis of a developmental circuit for direct transcriptional activation and repression in the same cell by a Runx protein. *Genes Dev.* **17**, 838-843.
Carey, M. (1998). The enhanceosome and transcriptional synergy. *Cell* **92**, 5-8.
Cinar, H. N., Richards, K. L., Oommen, K. S. and Newman, A. P. (2003). The EGL-13 SOX domain transcription factor affects the uterine pi cell lineages in Caenorhabditis elegans. *Genetics* **165**, 1623-1628.
Coffman, J. A. (2003). Runx transcription factors and the developmental balance between cell proliferation and differentiation. *Cell Biol. Int.* **27**, 315-324.
Crittenden, S. L., Eckmann, C. R., Wang, L., Bernstein, D. S., Wickens, M. and Kimble, J. (2003). Regulation of the mitosis/meiosis decision in the Caenorhabditis elegans germline. *Philos. Trans. R. Soc. Lond. B Biol. Sci.* **358**, 1359-1362.
Fire, A., Xu, S., Montgomery, M. K., Kostas, S. A., Driver, S. E. and Mello, C. C. (1998). Potent and specific genetic interference by double-stranded RNA in Caenorhabditis elegans. *Nature* **391**, 806-812.
Flemming, A. J., Shen, Z. Z., Cunha, A., Emmons, S. W. and Leroi, A. M. (2000). Somatic polyploidisation and cellular proliferation drive body size evolution in nematodes. *Proc. Natl. Acad. Sci. USA* **97**, 5285-5290.
Furger, A., Monks, J. and Proudfoot, N. J. (2001). The retroviruses human immunodeficiency virus type 1 and Moloney murine leukemia virus adopt radically different strategies to regulate promoter-proximal polyadenylation. *J. Virol.* **75**, 11735-11746.
Gengyo-Ando, K. and Mitani, S. (2000). Characterization of mutations induced by ethyl methanesulfonate, UV, and trimethylpsoralen in the nematode Caenorhabditis elegans. *Biochem. Biophys. Res. Commun.* **269**, 64-69.
Hobert, O. (2002). PCR fusion-based approach to create reporter gene constructs for expression analysis in transgenic *C. elegans*. *Biotechniques* **32**, 728-730.
Huang, G., Shigesada, K., Ito, K., Wee, H. J., Yokomizo, T. and Ito, Y. (2001). Dimerization with PEBP2beta protects RUNX1/AML1 from ubiquitin-proteasome-mediated degradation. *EMBO J.* **20**, 723-733.
Kagoshima, H., Sawa, H., Mitani, S., Burglin, T. R., Shigesada, K. and Kohara, Y. (2005). The C. elegans RUNX transcription factor RNT-1/MAB-2 is required for asymmetrical cell division of the T blast cell. *Dev. Biol.* **287**, 262-273.
Kagoshima, H., Shigesada, K. and Kohara, Y. (2007). RUNX regulates stem cell proliferation and differentiation: Insights from studies of *C. elegans*. *J. Cell. Biochem.* **100**, 1119-1130.
Keefe, A. D., Wilson, D. S., Seelig, B. and Szostak, J. W. (2001). One-step purification of recombinant proteins using a nanomolar-affinity streptavidin-binding peptide, the SBP-Tag. *Protein Expr. Purif.* **23**, 440-446.
Lee, J., Ahnn, J. and Bae, S. C. (2004). Homologs of RUNX and CBF beta/PEBP2 beta in C. elegans. *Oncogene* **23**, 4346-4352.
Li, Z., Yan, J., Matheny, C. J., Corpora, T., Bravo, J., Warren, A. J., Bushweller, J. H. and Speck, N. A. (2003). Energetic contribution of residues in the Runx1 Runt domain to DNA binding. *J. Biol. Chem.* **278**, 33088-33096.
Lutterbach, B., Hou, Y., Durst, K. L. and Hiebert, S. W. (1999). The inv(16) encodes an acute myeloid leukemia 1 transcriptional corepressor. *Proc. Natl. Acad. Sci. USA* **96**, 12822-12827.
Mello, C. and Fire, A. (1995). DNA transformation. In *Caenorhabditis elegans: Modern Biological Analysis of an Organism*. Vol. 48 (ed. D. Shakes and H. Epstein), pp. 451-482. San Diego: Academic Press.
Mitani, S. (1995). Genetic regulation of *mec-3* gene expression implicated in the specification of the mechanosensory neuron cell types in *Caenorhabditis elegans*. *Dev. Growth Differ.* **37**, 551-557.
Nagata, T. and Werner, M. H. (2001). Functional mutagenesis of AML1/RUNX1 and PEBP2 beta/CBF beta define distinct, non-overlapping sites for DNA recognition and heterodimerization by the Runt domain. *J. Mol. Biol.* **308**, 191-203.
Nam, S., Jin, Y. H., Li, Q. L., Lee, K. Y., Jeong, G. B., Ito, Y., Lee, J. and Bae, S. C. (2002). Expression pattern, regulation, and biological role of runt domain transcription factor, run, in Caenorhabditis elegans. *Mol. Cell. Biol.* **22**, 547-554.
Nimmo, R., Antebi, A. and Woollard, A. (2005). *mab-2* encodes RNT-1, a *C. elegans* Runx homologue essential for controlling cell proliferation in a stem cell-like developmental lineage. *Development* **132**, 5043-5054.
Pettitt, J., Wood, W. B. and Plasterk, R. H. (1996). cdh-3, a gene encoding a member of the cadherin superfamily, functions in epithelial cell morphogenesis in *Caenorhabditis elegans*. *Development* **122**, 4149-4157.
Pocock, R., Ahringer, J., Mitsch, M., Maxwell, S. and Woollard, A. (2004). A regulatory network of T-box genes and the even-skipped homologue *vab-7* controls posterior patterning and morphogenesis in *C. elegans*. *Development* **131**, 2373-2385.
Stein, G. S., Lian, J. B., van Wijnen, A. J., Stein, J. L., Montecino, M., Javed, A., Zaidi, S. K., Young, D. W., Choi, J. Y. and Pockwinse, S. M. (2004). Runx2 control of organization, assembly and activity of the regulatory machinery for skeletal gene expression. *Oncogene* **23**, 4315-4329.
Sulston, J. E. and Horvitz, H. R. (1977). Post-embryonic cell lineages of the nematode, Caenorhabditis elegans. *Dev. Biol.* **56**, 110-156.
Sulston, J. and Hodgkin, J. (1988). Methods. In *The Nematode Caenorhabditis elegans* (ed. W. B. Wood), pp. 587-606. Cold Spring Harbor, NY: Cold Spring Harbor Laboratory Press.
Sulston, J. E., Albertson, D. G. and Thomson, J. N. (1980). The Caenorhabditis elegans male: postembryonic development of nongonadal structures. *Dev. Biol.* **78**, 542-576.
Tahirov, T. H., Inoue-Bungo, T., Morii, H., Fujikawa, A., Sasaki, M., Kimura, K., Shiina, M., Sato, K., Kumasaka, T., Yamamoto, M. et al. (2001). Structural analyses of DNA recognition by the AML1/Runx-1 Runt domain and its allosteric control by CBFbeta. *Cell* **104**, 755-767.
Tanaka, J., Miwa, Y., Miyoshi, K., Ueno, A. and Inoue, H. (1999). Construction of Epstein-Barr virus-based expression vector containing mini-oriP. *Biochem. Biophys. Res. Commun.* **264**, 938-943.
Tanaka, Y., Watanabe, T., Chiba, N., Niki, M., Kuroiwa, Y., Nishihira, T., Satomi, S., Ito, Y. and Satake, M. (1997). The protooncogene product, PEBP2beta/CBFbeta, is mainly located in the cytoplasm and has an affinity with cytoskeletal structures. *Oncogene* **15**, 677-683.
Yan, J., Liu, Y., Lukasik, S. M., Speck, N. A. and Bushweller, J. H. (2004). CBFbeta allosterically regulates the Runx1 Runt domain via a dynamic conformational equilibrium. *Nat. Struct. Mol. Biol.* **11**, 901-906.